

## Dissociation of methane under high pressure

Guoying Gao,<sup>1,a)</sup> Artem R. Oganov,<sup>2,a)</sup> Yanming Ma,<sup>1,b)</sup> Hui Wang,<sup>1</sup> Peifang Li,<sup>1</sup> Yinwei Li,<sup>1</sup> Toshiaki Itaka,<sup>3</sup> and Guangtian Zou<sup>1</sup><sup>1</sup>State Key Lab of Superhard Materials, Jilin University, Changchun 130012, People's Republic of China<sup>2</sup>Department of Geosciences, Department of Physics and Astronomy, and New York Center for Computational Sciences, Stony Brook University, Stony Brook, New York 11794, USA and<sup>3</sup>Department of Geology, Moscow State University, 119992 Moscow, Russia<sup>3</sup>Computational Astrophysics Laboratory, RIKEN, 2-1 Hirosawa, Wako, Saitama 351-0198, Japan

(Received 15 May 2010; accepted 18 August 2010; published online 12 October 2010)

Methane is an extremely important energy source with a great abundance in nature and plays a significant role in planetary physics, being one of the major constituents of giant planets Uranus and Neptune. The stable crystal forms of methane under extreme conditions are of great fundamental interest. Using the *ab initio* evolutionary algorithm for crystal structure prediction, we found three novel insulating molecular structures with  $P2_12_12_1$ ,  $Pnma$ , and  $Cmcm$  space groups. Remarkably, under high pressure, methane becomes unstable and dissociates into ethane ( $C_2H_6$ ) at 95 GPa, butane ( $C_4H_{10}$ ) at 158 GPa, and further, carbon (diamond) and hydrogen above 287 GPa at zero temperature. We have computed the pressure-temperature phase diagram, which sheds light into the seemingly conflicting observations of the unusually low formation pressure of diamond at high temperature and the failure of experimental observation of dissociation at room temperature. Our results support the idea of diamond formation in the interiors of giant planets such as Neptune.

© 2010 American Institute of Physics. [doi:10.1063/1.3488102]

### I. INTRODUCTION

The high-pressure behavior of methane ( $CH_4$ ) is of great importance in view of the significant role it plays in planetary physics, being one of the major constituents of giant planets Uranus and Neptune, where it is subjected to pressures of up to 600 GPa and temperatures of several thousand Kelvin.<sup>1,2</sup> In spite of the simplicity of its molecule (the simplest saturated hydrocarbon),  $CH_4$  has a complex and poorly understood phase diagram.<sup>3–8</sup> At low temperature and low pressure,  $CH_4$  adopts a partially orientationally ordered cubic  $Fm3c$  structure (phase II),<sup>7</sup> and then transforms to an orientationally ordered orthorhombic  $Cmca$  phase (phase III)<sup>3</sup> at 0.02 GPa. At low temperature and slightly higher pressure,  $CH_4$  transforms to phases IV, V, and VI, structures of which have not been determined yet.<sup>5,6</sup> More interestingly, it is expected that  $CH_4$  becomes chemically unstable and undergoes a chemical disproportionation under high pressure.<sup>9</sup> Experiments conducted at high temperatures<sup>10,11</sup> have indeed observed this decomposition. However, room-temperature compression experiments on methane did not reveal its dissociation up to  $\sim 200$  GPa.<sup>12</sup> Neither the pressure of onset of its instability nor the products of methane's chemical transformation are well constrained. Some studies<sup>11,13–16</sup> suggested that  $CH_4$  decomposes into diamond and hydrogen (10–50 GPa), while others<sup>17</sup> proposed that it polymerizes into heavier hydrocarbons (below 100 GPa) before producing diamond and hydrogen on further increase of pressure.

Moreover, previous theoretical work<sup>17</sup> predicted that at high pressure and temperature,  $CH_4$  dissociates fully to form diamond only at pressures above 300 GPa, whereas the experiments<sup>10,11,13,15</sup> found that such a reaction proceeded at pressures as low as 10–50 GPa.

To give the specific decomposition pressure of methane, resolve the controversy over its decomposition product, and explore the possibility of its metallization and superconductivity under pressure, here we use an *ab initio* evolutionary algorithm Universal Structure Predictor: Evolutionary Xtallography (USPEX)<sup>18–20</sup> to explore the behavior of  $CH_4$  under high pressure ( $\geq 20$  GPa) and low temperatures. This method has proven its reliability and efficiency in predicting the stable structures with only the knowledge of the chemical composition. Many successful applications<sup>21–27</sup> have been described elsewhere. We find that on increasing pressure  $CH_4$  first keeps its molecular form, then it dissociates into ethane ( $C_2H_6$ ), butane ( $C_4H_{10}$ ), and finally, diamond mixed with hydrogen. We also establish a pressure-temperature phase diagram to explain the difference in the pressure of diamond formation in experiments at room and high temperatures.

### II. COMPUTATIONAL METHOD

*Ab initio* evolutionary simulations are used to search for the structure possessing the lowest free energy (i.e., the stable structure) and here we perform searches at zero temperature and different pressures, using no knowledge of any structural information. Evolutionary structure prediction was performed using the USPEX method/code.<sup>18–20</sup> The first generation of structures (population size: 20–50 structures, increasing with system size) was always produced randomly.

<sup>a)</sup>Electronic mail: gaoguoying1981@yahoo.com.cn; artem.oganov@sunysb.edu.

<sup>b)</sup>Author to whom correspondence should be addressed. Electronic mail: mym@jlu.edu.cn.

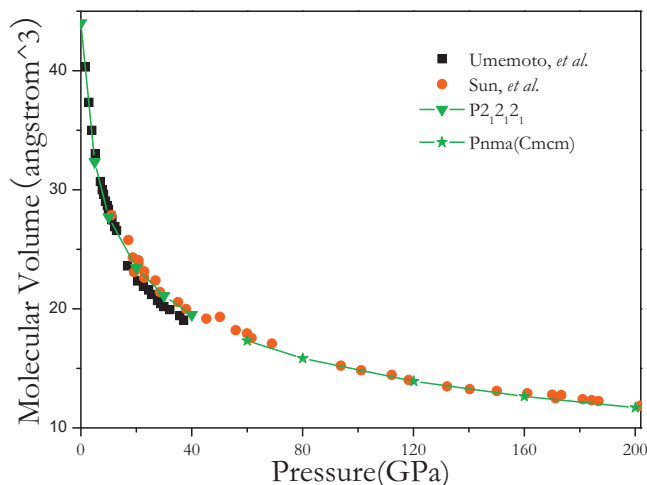


FIG. 1. The calculated equation of state compared with the experimental data (Refs. 4 and 12).

Every subsequent generation is produced from the best 60% of the previous generation. New structures are created by heredity (i.e., combining spatially coherent slabs cut from two parent structures in a random direction at random positions and with random thicknesses), permutation, and lattice mutation (with Gaussian strength 0.5–0.7). In addition, the best structure of each generation is carried over into the next generation. Numerous tests show that for systems with  $\sim 20$  atoms/cell the global minimum (which, for well-known test cases, is the experimentally known stable structure) is usually reached well within  $\sim 20$  generations ( $\sim 600$  local optimizations). The calculation stops when the best structure does not change for more than 20 generations. The underlying *ab initio* structure relaxations are performed using density functional theory within the Perdew–Burke–Ernzerhof generalized gradient approximation,<sup>28</sup> as implemented in the VASP (Vienna *Ab Initio* Simulation Package) code.<sup>29</sup> The all-electron projector-augmented wave<sup>30</sup> method was adopted, with a [He] core (radius 0.58 Å) for C atom and core region of 0.42 Å radius for the H atom. The use of the plane-wave kinetic energy cutoff of 520 eV and dense k-point sampling adopted here were shown to give excellent convergence of the energy differences and stress tensors.

### III. RESULTS AND DISCUSSION

We performed variable-cell structure prediction simulations for CH<sub>4</sub> with the cell sizes containing two to four formula units at 20, 60, 100, 200, and 300 GPa, and four formula units at 400, 600, and 800 GPa, respectively. Analyzing the results, we found that below 200 GPa, the low-enthalpy structures are all completely made of well-separated CH<sub>4</sub> molecules. Three novel orthorhombic structures with space groups  $P2_12_12_1$ ,  $Pnma$ , and  $Cmcm$ , all of which contain four formula units per cell, are uncovered for the first time. Their computed equation of state is in agreement with the experimental equation of state (Fig. 1).<sup>4,12</sup> In the  $P2_12_12_1$  structure [Fig. 2(a)], each CH<sub>4</sub> molecule forms a slightly distorted tetrahedron with C–H distances about 1.068–1.073 Å and H–C–H angles in the range 108.90°–110.54°. We note that the low-temperature phases of GeD<sub>4</sub> and SiD<sub>4</sub> reported by

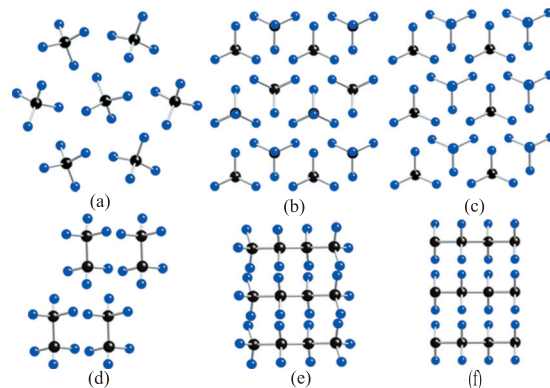


FIG. 2. (a)–(c) The predicted  $P2_12_12_1$ ,  $Pnma$ , and  $Cmcm$  structures of CH<sub>4</sub>. (d)–(f) The predicted structures of C<sub>2</sub>H<sub>6</sub>, C<sub>4</sub>H<sub>10</sub>, and CH<sub>2</sub> with space groups  $P-1$ ,  $P-1$ , and  $Cmcm$ , respectively. The large and small spheres represent C and H atoms, respectively.

the recent neutron experiment<sup>31</sup> also have the same  $P2_12_12_1$  structure. In the  $Pnma$  structure [Fig. 2(b)], CH<sub>4</sub> also keeps its molecular form, but the structural packing is denser (molecules take antiparallel orientations). If we rotate some of the molecules in the  $Pnma$  structure by 180°, then a  $Cmcm$  structure [Fig. 2(c)] is readily obtained. We also note that these structures have lower enthalpies than the recently found (Zhu & Oganov, unpublished) structures of plastic forms of methane experimentally seen in this pressure range at room temperature,<sup>12</sup> implying that the latter are metastable. Structural parameters of the  $P2_12_12_1$ ,  $Pnma$ , and  $Cmcm$  structures are listed in the supplementary material (SM).<sup>32</sup> The pressure variation of the enthalpies of the predicted structures is shown in Fig. 3. It should be pointed out that the enthalpy differences between the  $Pnma$  and  $Cmcm$  structures are only within a few meV/molecule. The stability fields of  $P2_12_12_1$ ,  $Pnma$ , and  $Cmcm$  structures are below 58 GPa, in the range of 58–138 GPa and above 138 GPa, respectively.

At and above 200 GPa, our structural simulations revealed surprisingly numerous low-enthalpy structures made of higher hydrocarbons [C<sub>2</sub>H<sub>6</sub>, propane C<sub>3</sub>H<sub>8</sub>, C<sub>4</sub>H<sub>10</sub>, and

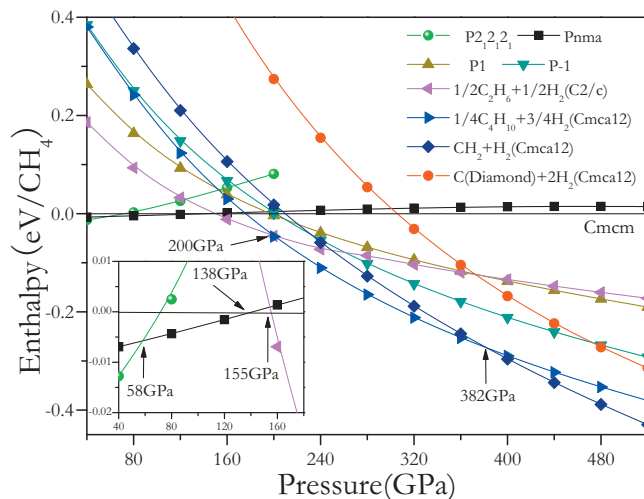


FIG. 3. Enthalpy curves (relative to our predicted  $Cmcm$  phase) for CH<sub>4</sub> as a function of pressure without the zero-point corrections.

TABLE I. The zero-point vibrational energies ( $E_{\text{ZP}}$ , electron volts/formula unit) for C (diamond),  $\text{H}_2$ ,  $\text{CH}_4$ ,  $\text{CH}_2$ ,  $\text{C}_2\text{H}_6$ , and  $\text{C}_4\text{H}_{10}$  at 200 GPa.

| Materials                 | Space group                 | Zero-point vibrational energy ( $E_{\text{ZP}}$ ) (eV/formula unit) |
|---------------------------|-----------------------------|---|
| C                         | <i>Fd-3m</i>                | 0.232   |
| $\text{H}_2$              | <i>C2/c</i> <sup>a</sup>    | 0.585   |
|                           | <i>Cmca_12</i> <sup>a</sup> | 0.584   |
| $\text{CH}_4$             | <i>P2_12_12_1</i>           | 1.686   |
|                           | <i>Pnma</i>                 | 1.693   |
|                           | <i>Cmcm</i>                 | 1.696   |
|                           | <i>P1</i>                   | 1.634   |
|                           | <i>P-1</i>                  | 1.600   |
| $\text{CH}_2$             | <i>Cmcm</i>                 | 0.983   |
| $\text{C}_2\text{H}_6$    | <i>P-1</i>                  | 2.686   |
| $\text{C}_4\text{H}_{10}$ | <i>P-1</i>                  | 4.637   |

<sup>a</sup>Reference 34.

infinite-chain  $(\text{CH}_2)_\infty$  polymer] mixed with  $\text{H}_2$  molecules (see Fig. SM1).<sup>32</sup> This clearly suggests the possibility of decomposition, and in the next step we looked for stable structures of alkanes  $\text{C}_2\text{H}_6$ ,  $\text{C}_3\text{H}_8$ ,  $\text{C}_4\text{H}_{10}$ , pentane ( $\text{C}_5\text{H}_{12}$ ), hexane ( $\text{C}_6\text{H}_{14}$ ), and infinite-chain polymer  $(\text{CH}_2)_\infty$  by performing additional evolutionary structural searches<sup>33</sup> and considered enthalpies of  $\text{CH}_4$  dissociation into these alkanes and hydrogen:<sup>34</sup>  $n\text{CH}_4 = \text{C}_n\text{H}_{2n+2} + (n-1)\text{H}_2$ . No molecular constraints were applied (as throughout this study) and it is gratifying that the predicted stable structures for the hydrocarbons are all completely made of their respective molecular forms except for  $\text{C}_3\text{H}_8$ , which is found to decompose into  $\text{C}_2\text{H}_6$  and  $\text{C}_4\text{H}_{10}$  mixed with  $\text{H}_2$ . The most stable structures for  $\text{C}_2\text{H}_6$ ,  $\text{C}_4\text{H}_{10}$ , and infinite-chain polymer  $(\text{CH}_2)_\infty$  are illustrated in Figs. 2(d)–2(f). After considering the enthalpy of dissociation, we found that  $\text{CH}_4$  dissociates into  $\text{C}_2\text{H}_6 + \text{H}_2$  at 155 GPa, then into  $\text{C}_4\text{H}_{10} + 3\text{H}_2$  at 200 GPa, and finally into  $\text{CH}_2 + \text{H}_2$  above 382 GPa (see Fig. 3). The enthalpy of decomposition into diamond and  $\text{H}_2$  is also included to examine the earlier theoretical prediction<sup>17</sup> and experimental discovery<sup>11</sup> of the existence of diamond under high pressure. However, it is found that the decomposition into the mixture of  $\text{C}_2\text{H}_6/\text{C}_4\text{H}_{10}/\text{CH}_2$  and  $\text{H}_2$  is more thermodynamically favorable, seemingly eliminating the formation of diamond by decomposition of methane under high pressure.

However, it is expected that quantum effects related to the zero-point (ZP) motion are large and could affect the relative structural stability for systems made of such light atoms. We have therefore estimated the ZP contribution (which includes both intermolecular and intramolecular vibrations) using direct phonon calculations<sup>35</sup> for various structures—these are listed in Table I for the pressure of 200 GPa. These phonon calculations (see the SM) (Ref. 32) also enabled us to check the dynamical stability of our predicted structures, all of which, indeed, have no imaginary phonon frequencies and are therefore dynamically stable. It is evident that the ZP energy is very large and could fundamentally revise phase stability (Table I). The phase transition sequence including the ZP energy can be seen in Fig. 4. It is found that with the inclusion of ZP motion, the stability fields of the *P2*<sub>1</sub>*2*<sub>1</sub>*2*<sub>1</sub> and *Pnma* structures have been shifted

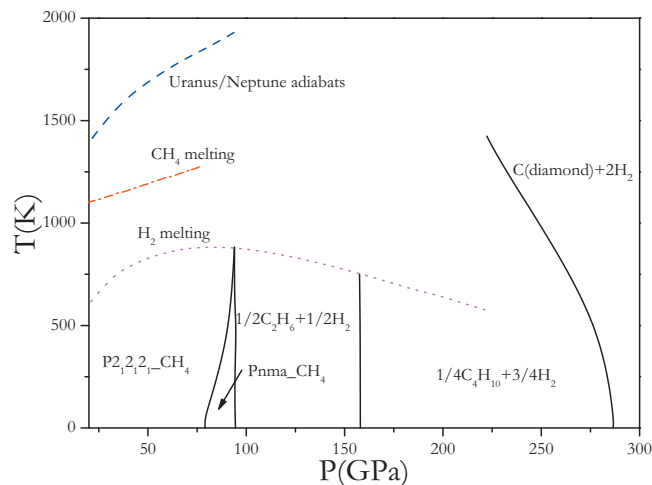


FIG. 4. The phase diagram of  $\text{CH}_4$  as a function of pressure and temperature. The solid lines are phase boundaries of different structures. The melting line of  $\text{CH}_4$  (the dashed-dotted line) (Ref. 10) and  $\text{H}_2$  (the dotted line) (Ref. 37), and Uranus/Neptune adiabats (the dashed line) (Ref. 44) are also shown.

to below 79 GPa and to the range 79–95 GPa, respectively. Although the addition of ZP effects has excluded the *Cmcm* structure as a stable phase in the enthalpy plots, the *Cmcm* structure could still be seen as a candidate phase between 79 and 95 GPa, as the enthalpy differences are small and could be within theoretical uncertainties. The ZP effects do not change the structural stability of  $\text{C}_2\text{H}_6 + \text{H}_2$  and  $\text{C}_4\text{H}_{10} + 3\text{H}_2$ , but modify their stable ranges to be 95–158 and 158–287 GPa, respectively. The most surprising and important result is that the mixture of diamond and hydrogen, unstable without accounting for ZP energy, does become stable once ZP energy is taken into account.  $\text{CH}_4$  is predicted to dissociate into diamond and  $\text{H}_2$  above 287 GPa and 0 K (Fig. 4). An earlier theoretical work<sup>17</sup> predicted the formation of diamond above 300 GPa at 0 K (without zero-point motion), due to a fortuitous error cancellation: on one hand, ZP energies were ignored; on the other hand, the structures used for the hydrocarbons were not the most stable ones, but highly disordered high-enthalpy structures found using molecular dynamics quenches. Our theoretical results, not suffering from such deficiencies, are in good agreement with the experimental observations<sup>10,11,13,15</sup> and for the first time predict the specific dissociation products and pressures. The main difference is the pressure at which diamond forms. Our predicted pressure is about 290 GPa, much higher than the experimental pressures of 10–50 GPa.<sup>10,11,13,15</sup> Note that our prediction was performed at 0 K temperature, while the experiments were done at least at 2000 K; the large difference in pressures is likely due to temperature effects (note that the large ZP energy differences come from very different phonon spectra of diamond, hydrogen, and various hydrocarbons; for the same reason, one should expect large entropy differences and large temperature effects on stability fields). To clarify this point, we have carefully calculated the phase diagram of  $\text{CH}_4$  at high pressures and temperatures within the quasiharmonic approximation (as we did in the previous work)<sup>36</sup> as shown in Fig. 4. Remarkably, this phase diagram implies that the formation pressure of diamond decreases sharply with

increasing temperature and is reduced to  $\sim 190$  GPa at 2000 K, the highest temperature considered here. We note also that the quasiharmonic approximation cannot be applied to fluids (and note that hydrogen melts at relatively low temperatures, e.g., Ref. 37) and that the formation of fluid phases will further decrease the pressure of dissociation (i.e., our calculated dissociation pressures are upper bounds). The remarkably large temperature effect on dissociation of methane allows us to understand discrepancies in experimental observations; high temperature experiments in diamond anvil cells<sup>10,11,13,15</sup> have observed dissociation into diamond and hydrogen at rather low pressures due to the strong decrease of decomposition pressure with temperature; the formation of diamond could also be eased by the use of diamond anvils and incomplete equilibrium achieved in experiments. It should be further noted that if the experiment is performed at low temperature, dissociation is likely to be kinetically hindered due to high activation barriers associated with bond breaking and making. This explains the failure to observe dissociation of methane up to 202 GPa in room-temperature experiments.<sup>12</sup>

The formation of diamond is likely to have a major impact on the energetics of the giant planet Neptune (which is known to have a mysterious internal heat production mechanism, necessary to explain its high luminosity): sinking of dense diamond inside the planet would release significant amounts of energy. Possible metallization of CH<sub>4</sub> under pressure is also of importance for understanding planetary magnetic fields and is interesting for fundamental reasons (viz., the recent proposal<sup>38</sup> that CH<sub>4</sub> will be a good superconductor, if it were a metal under high pressure). However, we find that our predicted ground-state  $P2_12_12_1$ ,  $Pnma$ , and  $Cmcm$  structures are all insulators (see the SM)<sup>32</sup> with wide band gaps that do not close up to pressures of at least 520 GPa, which is consistent with recent experiments<sup>39,40</sup> and earlier theoretical prediction.<sup>41</sup> While CH<sub>4</sub> itself does not metalize under pressure, hydrogen (formed as a result of decomposition CH<sub>4</sub> → C + 2H<sub>2</sub>) will be metallic at planetary conditions; its metallization was observed above 140 GPa and 3000 K<sup>42</sup> and at room temperature is expected to occur above 410 GPa.<sup>34</sup> Metallic hydrogen, released at decomposition of methane, is thus potentially important for magnetic fields of planets such as Neptune.

Since diamond, a decomposition product of methane, is denser than hydrogen and hydrocarbons, there should be gravitational sinking of diamond inside giant planets Neptune and possibly Uranus. However, C<sub>2</sub>H<sub>6</sub> and C<sub>4</sub>H<sub>10</sub> are unlikely to sink. They may partly leak into the atmosphere. Our results show that a considerable amount of C<sub>2</sub>H<sub>6</sub> and C<sub>4</sub>H<sub>10</sub> could exist in the middle ice layer. The abundance of atmospheric C<sub>2</sub>H<sub>6</sub> and C<sub>4</sub>H<sub>10</sub> could be understood in terms of a convective mechanism carrying C<sub>2</sub>H<sub>6</sub> and C<sub>4</sub>H<sub>10</sub> from the middle ice layer up to the observable atmosphere.<sup>43</sup> Encouragingly, C<sub>2</sub>H<sub>6</sub> was indeed found in Neptune's atmosphere.<sup>43</sup> The complex transformation products, such as C<sub>2</sub>H<sub>6</sub>, C<sub>4</sub>H<sub>10</sub>, diamond, and hydrogen, have to be realistically taken into account in the models of internal evolution and energetics of these planets.

## IV. CONCLUSIONS

In summary, we have systematically investigated the phase diagram of methane under pressure through *ab initio* evolutionary simulations. At low pressure, methane keeps its molecular state and adopts  $P2_12_12_1$  symmetry below 79 GPa. In the pressure range 79–95 GPa, two novel structures with space groups  $Pnma$  and  $Cmcm$  are found to be the most promising candidates. Under higher pressure, methane becomes unstable and dissociates into the mixtures of C<sub>2</sub>H<sub>6</sub> and C<sub>4</sub>H<sub>10</sub> with hydrogen below 287 GPa, and into a diamond+hydrogen mixture above 287 GPa. Our computed pressure-temperature phase diagram explains conflicting experimental observations: the observed unusually low formation pressure of diamond at high temperature and the failure of experimental observation of dissociation at room temperature. In addition, our results also show that methane remains insulating up to very high pressures, which provides strong evidence for the impossibility of this compound to be a superconductor at pressures reachable with current static high-pressure techniques.

## ACKNOWLEDGMENTS

G.G. and Y.M. are thankful for financial support from the National Natural Science Foundation of China (NSFC) under Grant Nos. 10874054, 11025418 and 91022029, the NSFC awarded Research Fellowship for International Young Scientists (Grant No. 10910263), the China 973 Program (Grant No. 2005CB724400), the research fund for Excellent Young Scientist in Jilin University (Grant No. 200905003), and the 2007 Cheung Kong Scholars Program of China. G.G. is also grateful to the Project No. 20092004 supported by Graduate Innovation Fund of Jilin University. A.R.O. gratefully acknowledges funding from DARPA (Award No. 54751), Intel Corp., Rosnauka (Russia, Contract No. 02.740.11.5102), Research Foundation of Stony Brook University, and the New York Center for Computational Sciences and Joint Supercomputer Center (Russian Academy of Science, Moscow) for access to supercomputers. T.I. acknowledges the MEXT Grant (Grant No.20103005) and access to the computing facilities at RSCC system in RIKEN (Japan).

<sup>1</sup>W. B. Hubbard, W. J. Nellis, A. C. Mitchell, N. C. Holmes, S. S. Limaye, and P. C. McCandless, *Science* **253**, 648 (1991).

<sup>2</sup>W. B. Hubbard and J. J. MacFarlane, *J. Geophys. Res.* **85**, 225 (1980).

<sup>3</sup>M. A. Neumann, W. Press, C. Nöldeke, B. Asmussen, M. Prager, and R. M. Ibberson, *J. Chem. Phys.* **119**, 1586 (2003).

<sup>4</sup>S. Umamoto, T. Yoshii, Y. Akahama, and H. Kawamura, *J. Phys.: Condens. Matter* **14**, 10675 (2002).

<sup>5</sup>R. Bini and G. Pratesi, *Phys. Rev. B* **55**, 14800 (1997).

<sup>6</sup>R. Bini, L. Ulivi, H. J. Jodl, and P. R. Salvi, *J. Chem. Phys.* **103**, 1353 (1995).

<sup>7</sup>W. Press, *J. Chem. Phys.* **56**, 2597 (1972).

<sup>8</sup>R. M. Hazen, H. K. Mao, L. W. Finger, and P. M. Bell, *Appl. Phys. Lett.* **37**, 288 (1980).

<sup>9</sup>M. Ross, *Nature (London)* **292**, 435 (1981).

<sup>10</sup>H. Hirai, K. Konagai, T. Kawamura, Y. Yamamoto, and T. Yagi, *Phys. Earth Planet. Inter.* **174**, 242 (2009).

<sup>11</sup>L. R. Benedetti, J. H. Nguyen, W. A. Caldwell, H. J. Liu, M. Kruger, and R. Jeanloz, *Science* **286**, 100 (1999).

<sup>12</sup>L. L. Sun, W. Yi, L. Wang, J. F. Shu, S. Sinogeikin, Y. Meng, G. Y. Shen, L. G. Bai, Y. C. Li, J. Liu, H. K. Mao, and W. L. Mao, *Chem. Phys. Lett.*

- 473, 72 (2009).
- <sup>13</sup> A. Zerr, G. Serghiou, R. Boehler, and M. Ross, *High Press. Res.* **26**, 23 (2006).
- <sup>14</sup> W. J. Nellis, D. C. Hamilton, and A. C. Mitchell, *J. Chem. Phys.* **115**, 1015 (2001).
- <sup>15</sup> W. J. Nellis, F. H. Ree, M. van Thiel, and A. C. Mitchell, *J. Chem. Phys.* **75**, 3055 (1981).
- <sup>16</sup> M. Ross and F. H. Ree, *J. Chem. Phys.* **73**, 6146 (1980).
- <sup>17</sup> F. Ancilotto, G. L. Chiarotti, S. Scandolo, and E. Tosatti, *Science* **275**, 1288 (1997).
- <sup>18</sup> A. R. Oganov, C. W. Glass, and S. Ono, *Earth Planet. Sci. Lett.* **241**, 95 (2006).
- <sup>19</sup> A. R. Oganov and C. W. Glass, *J. Chem. Phys.* **124**, 244704 (2006).
- <sup>20</sup> C. W. Glass, A. R. Oganov, and N. Hansen, *Comput. Phys. Commun.* **175**, 713 (2006).
- <sup>21</sup> Y. M. Ma, Y. C. Wang, and A. R. Oganov, *Phys. Rev. B* **79**, 054101 (2009).
- <sup>22</sup> A. R. Oganov, J. H. Chen, C. Gatti, Y. Z. Ma, Y. M. Ma, C. W. Glass, Z. X. Liu, T. Yu, O. O. Kurakevych, and V. L. Solozhenko, *Nature (London)* **457**, 863 (2009).
- <sup>23</sup> Y. M. Ma, A. R. Oganov, Z. W. Li, Y. Xie, and J. Kotakoski, *Phys. Rev. Lett.* **102**, 065501 (2009).
- <sup>24</sup> Y. M. Ma, M. Eremets, A. R. Oganov, Y. Xie, I. Trojan, S. Medvedev, A. O. Lyakhov, M. Valle, and V. Prakapenka, *Nature (London)* **458**, 182 (2009).
- <sup>25</sup> G. Y. Gao, A. R. Oganov, A. Bergara, M. Martinez-Canales, T. Cui, T. Iitaka, Y. M. Ma, and G. T. Zou, *Phys. Rev. Lett.* **101**, 107002 (2008).
- <sup>26</sup> Q. Li, Y. M. Ma, A. R. Oganov, H. B. Wang, H. Wang, Y. Xu, T. Cui, H. K. Mao, and G. T. Zou, *Phys. Rev. Lett.* **102**, 175506 (2009).
- <sup>27</sup> G. Y. Gao, A. R. Oganov, P. F. Li, Z. W. Li, H. Wang, T. Cui, Y. M. Ma, A. Bergara, A. O. Lyakhov, T. Iitaka, and G. T. Zou, *Proc. Natl. Acad. Sci. U.S.A.* **107**, 1317 (2010).
- <sup>28</sup> J. P. Perdew, K. Burke, and M. Ernzerhof, *Phys. Rev. Lett.* **77**, 3865 (1996).
- <sup>29</sup> G. Kresse and J. Furthmüller, *Phys. Rev. B* **54**, 11169 (1996).
- <sup>30</sup> P. E. Blöchl, *Phys. Rev. B* **50**, 17953 (1994).
- <sup>31</sup> I. J. Maley, D. H. Brown, R. M. Ibberson, and C. R. Pulham, *Acta Crystallogr., Sect. B: Struct. Sci.* **64**, 312 (2008).
- <sup>32</sup> See supplementary material at <http://dx.doi.org/10.1063/1.3488102> for the computational details, calculated structure parameters, phonon dispersion curves, electronic band structure, and the band gap.
- <sup>33</sup> (CH<sub>2</sub>)<sub>z</sub> (two, four, and six formula units per cell at 300 GPa and six formula units per cell at 800 GPa), C<sub>4</sub>H<sub>10</sub> (one and two formula units per cell at 300 and 800 GPa), C<sub>2</sub>H<sub>6</sub>, C<sub>3</sub>H<sub>8</sub> (one and two formula units per cell at 300 GPa), C<sub>5</sub>H<sub>12</sub> and C<sub>6</sub>H<sub>14</sub> (one formula unit per cell at 300 GPa).
- <sup>34</sup> C. J. Pickard and R. J. Needs, *Nat. Phys.* **3**, 473 (2007).
- <sup>35</sup> Y. M. Ma and J. S. Tse, *Solid State Commun.* **143**, 161 (2007).
- <sup>36</sup> Y. Xu, L. J. Zhang, T. Cui, Y. Li, Y. Xie, W. Yu, Y. M. Ma, and G. T. Zou, *Phys. Rev. B* **76**, 214103 (2007).
- <sup>37</sup> S. Deemyad and I. F. Silvera, *Phys. Rev. Lett.* **100**, 155701 (2008).
- <sup>38</sup> N. W. Ashcroft, *Phys. Rev. Lett.* **92**, 187002 (2004).
- <sup>39</sup> L. L. Sun, Z. X. Zhao, A. L. Ruoff, C. S. Zha, and G. Stupian, *J. Phys.: Condens. Matter* **19**, 425206 (2007).
- <sup>40</sup> A. L. Ruoff (private communication).
- <sup>41</sup> M. Martinez-Canales and A. Bergara, *High Press. Res.* **26**, 369 (2006).
- <sup>42</sup> S. T. Weir, A. C. Mitchell, and W. J. Nellis, *Phys. Rev. Lett.* **76**, 1860 (1996).
- <sup>43</sup> J. I. Moses, K. Rages, and J. B. Pollack, *Icarus* **113**, 232 (1995).
- <sup>44</sup> I. de Pater and J. J. Lissauer, *Planetary Sciences* (Cambridge University Press, Cambridge, 2001), p. 215.